BORNEO JOURNAL OF SCIENCES AND TECHNOLOGY (BJoST)
VOL. : 7, ISSUE: 2, 72-80
DOI: http://doi.org/10.35370/bjost.2025.7.2-05
e-ISSN: 2672-7439 © 2018, UTS Publisher.

University of Technology Sarawak

ORIGINAL ARTICLE

Flow Analysis around Kuching Barrage by Field Measurement and Large Eddy Simulation Turbulence Model Using 3D Computational Fluid Dynamics

[1]Nurul Izzah Khairil Anuar, [*1]Saerahany Ibrahim, [3]Nik Mohd Kamel Nik Hassan, [1]Izihan Ibrahim, and [2]Zahir Ramli

[1]Department of Civil Engineering, International Islamic University Malaysia, 53100, Kuala Lumpur, Malaysia
[2]Institute of Oceanography and Maritime Studies (INOCEM), IIUM, 25200, Kuantan, Pahang, Malaysia
[3]Dr. Nik & Associates Sdn. Bhd., No 22 & 24, Jalan Wangsa Delima 6, Seksyen 5, Pusat Bandar Wangsa Maju, 53300 Kuala Lumpur, Malaysia

ABSTRACT – This study investigates the hydrodynamic complexity of turbulent flow conditions near the Kuching Barrage in the Sarawak River using field measurements and 3D Computational Fluid Dynamics (CFD) simulations FLOW-3D. Upstream and downstream of the barrage, Acoustic Doppler Current Profilers (ADCPs) were used to collect field data, which was then incorporated into a Large Eddy Simulation (LES) model to simulate the hydrodynamic properties. Riverbed surveys and sediment sampling enabled the model's implementation. The results showed good agreement between the modeled and measured data, providing evidence of the simulation's accuracy. It was demonstrated in the study that 3D modeling is essential for resolving complex dynamics associated with flow, which cannot be adequately addressed by conventional 1D or 2D methods. To improve the validity of future studies, future measurements should be prioritized, and finer computational grids should be more implemented.

ARTICLE HISTORY
Received: 21 Jan 2025
Revised: 03 Mar 2025
Accepted: 25 Apr 2025
Published: 31 July 2025

KEYWORDS
ADCP,
CFD modelling,
LES turbulence model,
Barrage,
Kuching River.

INTRODUCTION

With 30 nautical miles (52 kilometres) from the sea, Kuching is divided into northern and southern zones encompassing both urban and suburban areas. In these zones, tidal intrusion is observed, particularly during the "King Tides," which occurs after a new or full moon. It is estimated that the Highest Astronomical Tide (HAT) in the area reaches 6.5 meters (+2.5 meters above Mean Sea Level), the highest in Southeast Asia. It is not uncommon for low-lying areas to be affected by these tides, which occur on a monthly and fortnightly basis. In 1995, the Sarawak State Government introduced the Sungai Sarawak Regulation Scheme (SSRS). According to Figure 1, the scheme includes a barrage, a shiplock, and a bridge at the confluence of North Junction Point and Cameron Point.

Studying the complex flow and changes in river shape is important for keeping rivers safe for navigation and solving problem areas. This study focused on a 1-km stretch of the river bypass with the Kuching Barrage set to the center, using a combination of field measurements and 3D CFD modeling. Two Acoustic Doppler Current Profiler (ADCP) were employed 350 meters and 240 meters upstream and downstream of the barrage respectively to capture detailed flow measurements (Figure 2). 3D turbulence model, supported by high-resolution digital terrain data from recent riverbed scans, were also developed and tested. The primary objective is to determine whether such complex flow patterns can be accurately measured and reproduced using LES model governed by the CFD used. The study highlights the potential of these tools to model key variables such as velocity profiles and flow patterns.

*Corresponding Author: Saerahany Ibrahim. International Islamic University Malaysia (IIUM),
Email: saerahany@iium.edu.my

Figure 1. Kuching Barrage, Sarawak

Figure 2. Location of Deployed Device

MATERIALS AND METHODOLOGY

Large Eddy Simulation (LES)

Computational power is often required to accurately simulate turbulent flow. To reduce computing time while maintaining or improving accuracy, the problem is simplified in computational fluid dynamics (CFD) simulations. Large eddy simulations (LES) is a powerful CFD technique used to model turbulent flows in various environments, including rivers. First proposed by Joseph Smagorinsky in 1963 to simulate

atmospheric air currents, it was explored significantly by Deardorff in 1970. LES prioritizes the simulation of larger eddies influenced by flow geometry, while smaller, universal scales are modeled using a subgrid-scale (SGS) model [1]. This approach is based on Kolmogorov's 1941 self-similarity theory, which highlights how larger eddies are shaped by flow geometry, while smaller scales exhibit universality [2; 3]. LES employs the Navier-Stokes equations, foundational in fluid dynamics, to model fluid behavior. These equations address three core conservation principles. First, the conservation of mass ensures that the total fluid mass remains unchanged, regardless of movement or deformation [4; 5]. Second, the conservation of momentum, rooted in Newton's second law, maintains that the momentum within the fluid system remains constant over time. Lastly, the conservation of energy guarantees that the total energy of an isolated system is preserved, as stated by the first law of thermodynamics.

A key component of LES is its filtering process, which simplifies the complex Navier-Stokes equations. The filtering kernel identifies and emphasizes the larger eddies—the primary drivers of turbulent flow patterns—while averaging out the smaller, more universal scales [6]. This process uses a mathematical operation called convolution, which smooths the fluid's characteristics over a specific scale. In LES, the filtering operation is mathematically represented through an integral form, enabling precise modeling of large-scale turbulence effects while reducing computational demands [8].

$$\overline{\{\phi\}}(x,t) = \int_{\{-\infty\}}^{\{+\infty\}} \int_{\{-\infty\}}^{\{+\infty\}} \phi(r,\tau) G(x-r, t-\tau) dr d\tau \quad (1)$$

In the context of filtering operations in LES, $\overline{\{\phi\}}(x,t)$ represents the filtered field variable, which can signify quantities like velocity or pressure at a specific point x and time t. The unfiltered field variable, $\phi(r,\tau)$, captures the raw data at position r and time t. The filtering process is facilitated by a kernel, $G(x-r,t-\tau)$, which is applied to the field variable to emphasize specific scales. The double integral used in this process applies the filtering over all space and time, with dr and $d\tau$ serving as the differential elements for integration. This operation smooths out the smaller scales while retaining the essential larger eddy structures. After filtering in LES, the field variable ϕ is divided into two components. The filtered component ($\bar{\phi}$) represents the larger-scale part of the flow, capturing the averaged effects across larger eddies and structures, which are the focus of LES [9]. Meanwhile, the subgrid-scale component (ϕ') accounts for the smaller scales of motion, including tiny eddies and fluctuations that are too small to be resolved by the filter [10]. Together, these components combine to define the total field variable as:

$$\phi = \bar{\phi} + \phi' \quad (2)$$

where the filtered component reflects the resolved flow, and the subgrid-scale component represents the modeled effects.

Case Study

An established digital terrain model must be produced to initiate a CFD model. The survey used a GeoAcoustics 159D Dual Frequency SSS System with data acquisition software. SSS images were produced using narrow beams of acoustic energy transmitted from both sides of the tow fish across the seabed. The transmitted beams were characterized by narrow horizontal angles (1-2°), wide vertical angles (40-50°), and a pulse duration of less than 1 milliseconds. Acoustic energy reflected from the seabed and objects were detected by the tow fish. Sonar data quality depended on transverse resolution (affected by slant range and transducer beam width) and range resolution (influenced by acoustic velocity, grazing angle, and pulse width).

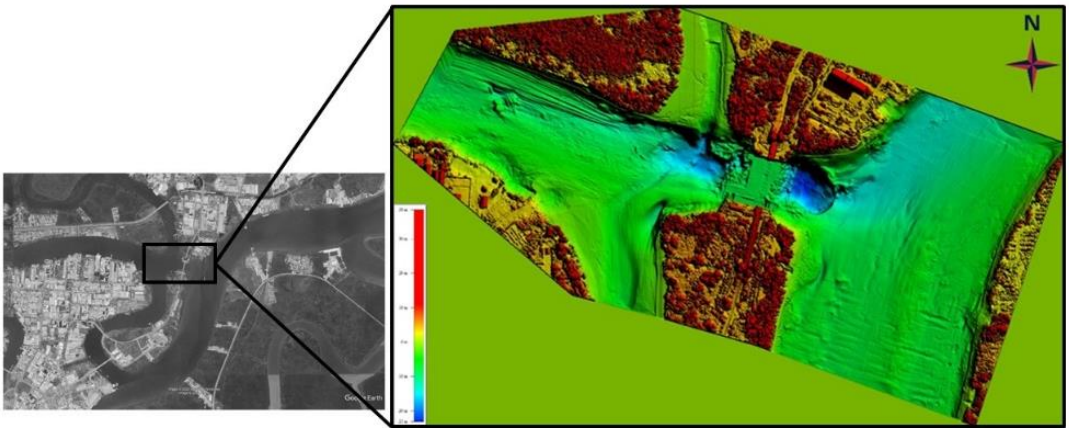

Figure 3. Processed Bathymetry of Kuching Barrage area

To explore to some extent, the distribution of bed surface material and its texture in space and time, field sampling started in January 2024 by applying a Van der Veen grab sampler at 14 designated locations, as shown in Figure 4(a). Each sample, weighing at least 1 kg, was stored in a clear plastic bag, double-bagged, tied, and labeled. The samples were sent to an accredited laboratory for particle size distribution analysis using the wet sieving method, including hydrometer tests where necessary, in accordance with BS1377: Part 2:1990 or ASTM D422-63(2007) (Figure 4(b)).

(a)

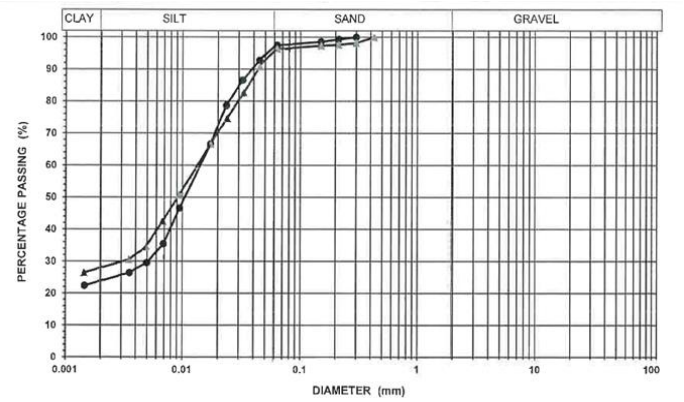

(b)

Figure 4. (a) Bed material sample and (b) Grain size distribution

Current measurements were taken using an Acoustic Doppler Current Profiler (ADCP) over 15 days. Speed and direction were recorded every 10 minutes, with data collected vertically from the riverbed to the water surface at 0.5 m intervals, including ~0.5 m above the seabed. Water depth, time, and location were noted during ADCP deployment and recovery. Measurements covered both neap and spring tides and ran alongside water level monitoring where the upstream, downstream and barrage area were also collected. Riverine discharge was measured at two cross-sections 3 days during both spring and neap tides. Where the measurements were taken hourly from 6:00 AM to 6:00 PM.

Computational Fluid Modelling (CFD)

The domain used for these simulations extends 450 m both up- and downriver of the barrage. The data was converted into a format that is compatible with the FLOW-3D software i.e., as stereolithography (.stl) where all the dimensions were scaled 1:1 with the site. The land mass was assumed as flat due to insufficient data as the survey was unable to cover the entire the flood plain, which is substantially large. The riverbanks were raised to contain spilling (Figure 5(b)). Figure 5(a) shows a scaled 3D model of the barrage structure. The dimensions were based on the As-Built drawings where the solid model was prepared using the SketchUp software that has the option to export solid sketches into 'stl' format.

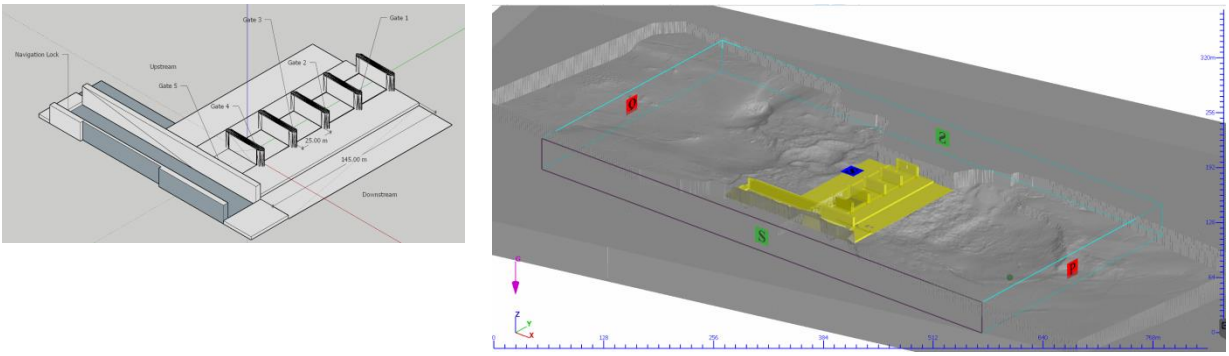

(a) (b)

Figure 5. a) The barrage structure prepared in 'stl' format and b) Model bathymetry with boundaries prepared in FLOW-3D

As seen in Figure 5(b), the boundaries of the model were defined. The volume flow rate (Q) boundary condition at Xmin distributes the total flow rate uniformly over the open surface, adjusting for changes in the surface area over time. The symmetry (S) condition at Ymin, Ymax, Zmin, Zmax applies a zero-gradient and zero-velocity condition, while the pressure (P) boundary at Xmax specifies pressure and fluid elevation, following a hydrostatic distribution.

FLOW-3D offers two mesh types: cylindrical and Cartesian, with Cartesian mesh selected for this study. A uniform grid is generated unless additional mesh planes are specified, which can adjust cell sizes or numbers. To manage stability and resolution, a single mesh block was used, with a cell size of 2.5 m and a total of 561,792 cells. A cell size of 2.5m provides a sufficient level of detail while avoiding excessive resource consumption, which is crucial for large-scale simulations. The Sungai Sarawak Barrage geometry was created in SketchUp and imported into FLOW-3D, where the FAVOR method embedded it into the computational grid by computing open area and volume fractions. This method simplifies the representation of complex surfaces but cannot resolve features smaller than the cell size. Geometry accuracy improves as mesh resolution increases, as shown in Figures 6.

The upstream ADCP measurement was carried out giving a discharge of 613.10 m3/s, before the flow approached the barrage to input as the flow ate boundary condition at Xmin (Figure 5b)). The downstream boundary the water level was set to the value belonging to this discharge according to the water level measured at site. Once setting the boundary conditions, the model was run until steady-state was reached. Another key model input to be considered is the parameterization of the bed roughness. To define this hydraulic resistance feature, the CFD model offers several options, out of which k_s, roughness height was implemented by using the $k_s = 3 \cdot d_{50}$.

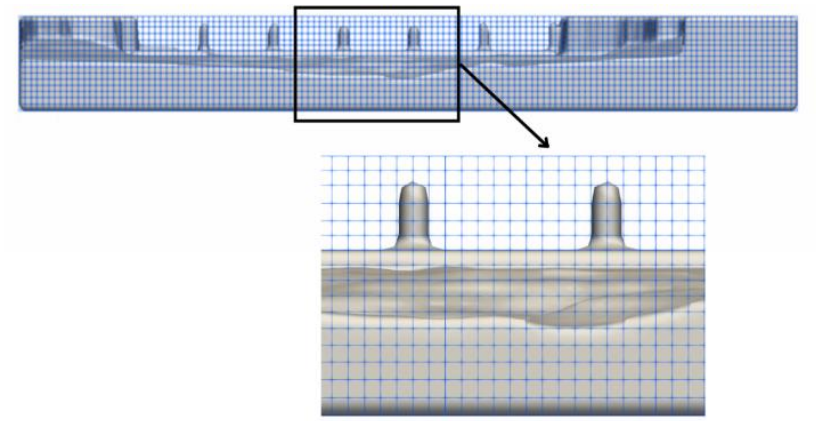

Figure 6. Sungai Sarawak Barrage front view created using FAVOR (top) and zoomed in at Gate 4 (bottom).

RESULTS AND DISCUSSION

The depth-averaged velocity magnitude distribution in the region of the Kuching Barrage is displayed in Figure 7. There are 4 divided zones: (1) stagnant zone; (2) bank separation zone; (3) deflection zone where the rapid flows passing the gates of the barrage meet showing patterns of deflecting towards the right bank; and (4) the acceleration zone where the upstream flow approaches the barrage. The white line indicates the cross-sectional region of where the ADCP was deployed at site (triangle on Figure 7). The ADCP data shows a lower velocity due to energy dissipation 200 meters further down the acceleration zone which was successfully captured by the simulation.

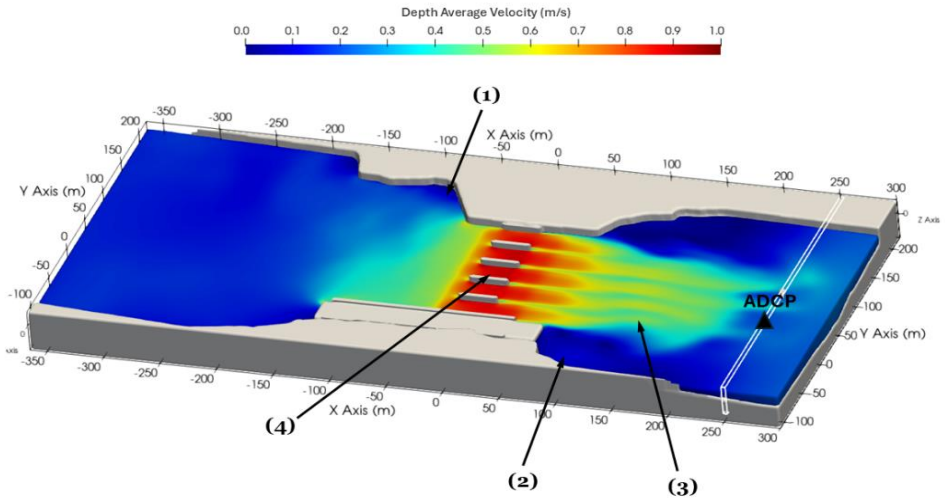

Figure 7. Depth Average Velocity Magnitude of Kuching Barrage

Shown in Figure 8, a distributed cross-section of the corresponding ADCP was used where the numerical modelling results can be compared and validated. In a steady-state simulation, velocity changes over time are not visible because they are included as part of the turbulent kinetic energy [11]. However, ADCP measurements can detect these velocity changes due to the rapid measurement technology that was utilized [12]. To match this behavior in the model, a method from [13] was used. It applies to a statistical relationship between turbulent kinetic energy and sudden velocity changes to calculate extra terms needed for a more accurate simulation.

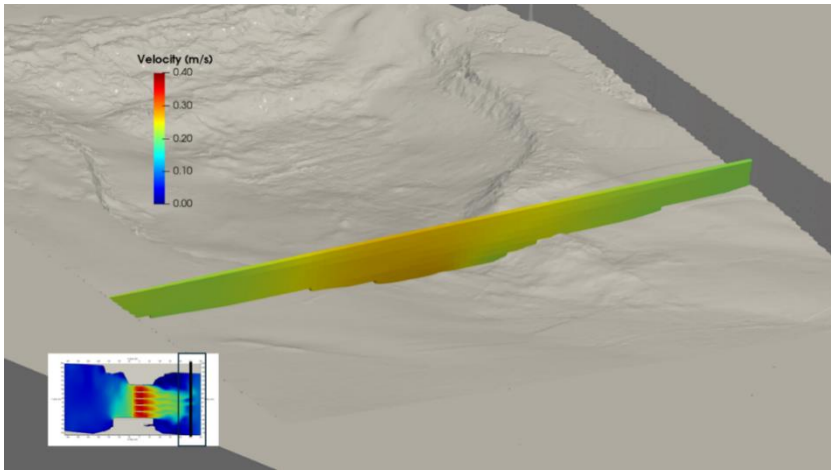

Figure 8. Modelled velocity magnitudes in the selected cross-section

In Figure 8, the secondary flow pattern in the cross-section can be seen when the main flow velocity (going perpendicular to that section) is removed. In a meandering channel, this secondary flow forms a swirling motion, as shown in Figure 9. This may be caused by uneven vertical velocity distribution. A bent vortex forms because the centrifugal force is stronger in the upper part of the flow than in the lower part. This creates a turning effect that causes circulation in the cross-section (Figure 9). Since flow speed decreases with depth, the upper layer experiences more centrifugal force than the lower layer, which explains the swirling pattern [13; 14].

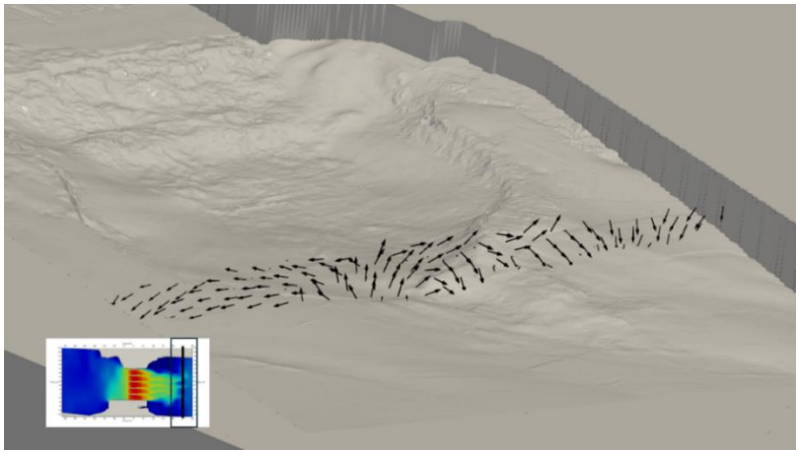

Figure 9. Secondary flow pattern in the plane perpendicular to the riverbed, showing velocity vector components

Figure 10 below illustrates the model results for two selected locations at 12 points vertically. A circle represents the result of a field measurement conducted by ADCP. Neither model result nor ADCP velocity profile exhibits a particularly steep logarithmic curve. With the fast-measuring capability of the ADCP, deviations between time averaged and instantaneous values may be high, but these values agree well with time averaged, steady-state measurements. As seen in Figure 10, the simulated model shows a fairly good agreement with the ADCP results in terms of the velocity profile. The error analysis shows that the model's performance is relatively strong, with an R^2 value of 81.31%, indicating that the model explains over 81% of the variance in the observed data. This suggests a good fit between the predicted and actual values, with the model capturing the majority of the underlying trend. Although further refinement is possible, the high R^2 value reflects the model's overall reliability in representing the field measurements.

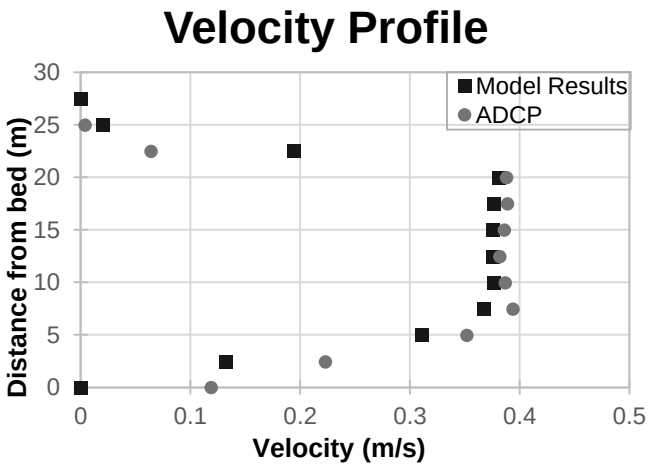

Figure 10. Vertical velocity profile

CONCLUSION

The simulation shows that LES is a useful tool for planning and designing future barrages and hydraulic structures, as it helps assess their impact on water flow and riverbed changes. The accuracy of LES depends on the quality of input data, such as water discharge, riverbank and bed shapes, and water levels. Advanced tools like 3D multibeam scanning can improve this data by providing better details on bed roughness, though collecting such data is costly and time-consuming [15]. LES also requires significant computing power, making it suitable only when high detail is essential—such as studying local flow and sediment transport, or predicting scouring during extreme floods to prevent structure failure. Simpler 1D or 2D models cannot capture this level of detail, and using 3D-RANS models is difficult due to the complex nature of hydraulic structures. LES is especially valuable for estimating turbulent kinetic energy (TKE) and scour depth. Higher accuracy in LES can be achieved with finer computational grids; in this study, the vertical resolution is about 2.5 meters.

ACKNOWLEDGEMENT

Computational work was performed at the Navier Stokes Domain Lab, Department of Civil Engineering, IIUM Gombak Malaysia. The visualization of a large dataset that was majorly contributed to this research was made possible by Dr. Nik & Associates Sdn. Bhd.

CONFLICTS OF INTEREST

The authors declare no conflict of interest.

REFERENCES

[1] J. Mathew, R. Lechner, H. Foysi, J. Sesterhenn, and R. Friedrich, “An explicit filtering method for large eddy simulation of compressible flows,” *Physics of Fluids*, vol. 15, no. 8, pp. 2279–2289, 2003, doi: 10.1063/1.1586271.

[2] Andrea. De Bortoli, G. S. L. . Andreis, and F. N. . Pereira, *Modeling andsimulation of reactive flows*. Elsevier, 2015. Accessed: Dec. 06, 2024. [Online]. Available: http://www.sciencedirect.com:5070/book/9780128029749/ modeling-and-simulation-of-reactive-flows

[3] J. Blazek and J. Blazek, *Chapter 7 – Turbulence Modeling*. 2015. Accessed: Dec. 06, 2024. [Online]. Available: http://www.sciencedirect.com:5070/book/9780080999951/computational-fluid-dynamics-principles-and-applications

[4] J. M. Rodríguez and R. Taboada-Vázquez, "A new LES model derived from generalized Navier-Stokes equations with nonlinear viscosity," *Comput. Math. Appl.*, vol. 73, no. 2, pp. 294–303, Jan. 2017, doi: 10.1016/J.CAMWA.2016.11.024.

[5] J. V. Gutiérrez-Santacreu and M. A. Rojas-Medar, "On the approximation of turbulent fluid flows by the Navier–Stokes-α equations on bounded domains," *Physica D*, vol. 448, Jun. 2023, doi: 10.1016/J.PHYSD.2023.133724.

[6] D. Oberle, C. D. Pruett, and P. Jenny, "Effects of time-filtering the Navier-Stokes equations," *Physics of Fluids*, vol. 35, no. 6, Jun. 2023, doi: 10.1063/5.0152642/17987156/065112_1_5.0152642.PDF.

[7] S. Stolz and N. A. Adams, "An approximate deconvolution procedure for large-eddy simulation," *Physics of Fluids*, vol. 11, no. 7, pp. 1699–1701, 1999, doi: 10.1063/1.869867.

[8] S. Stolz, N. A. Adams, and L. Kleiser, "An approximate deconvolution model for large-eddy simulation with application to incompressible wall-bounded flows," *Physics of Fluids*, vol. 13, no. 4, pp. 997–1015, 2001, doi: 10.1063/1.1350896.

[9] U. Piomelli, "Large-eddy simulation: achievements and challenges," *Progress in Aerospace Sciences*, vol. 35, no. 4, pp. 335–362, 1999, doi: 10.1016/S0376-0421(98)00014-1.

[10] S. Legare and M. Stastna, "Large eddy simulation analysis of a model reactive tracer through spatial filtering," *Phys Fluids*, vol. 36, no. 9, Sep. 2024, doi: 10.1063/5.0226039.

[11] M. Schröder, T. Bätge, E. Bodenschatz, M. Wilczek, and G. Bagheri, "Estimating the turbulent kinetic energy dissipation rate from one-dimensional velocity measurements in time," *Atmos Meas Tech*, vol. 17, no. 2, pp. 627–657, Jan. 2024, doi: 10.5194/AMT-17-627-2024.

[12] E. A. Nystrom, C. R. Rehmann, and K. A. Oberg, "Evaluation of mean velocity and turbulence measurements with ADCPs," *Journal of Hydraulic Engineering*, vol. 133, no. 12, pp. 1310–1318, Dec. 2007, doi: 10.1061/(ASCE)0733-9429(2007)133:12(1310).

[13] S. Baranya and J. Jozsa, "(PDF) Flow analysis in river Danube by field measurement and 3D CFD turbulence modelling," *PERIODICA POLYTECHNICA SER. CIV. ENG*, vol. 50, no. 1, 2006, Accessed: Dec. 18, 2024. [Online]. Available: https://www.researchgate.net/publication/228984532_Flow_analysis_in_river_Danube_by_field_measurement_and_3D_CFD_turbulence_modelling

[14] K. Shiono and Y. Muto, "Complex flow mechanisms in compound meandering channels with overbank flow," *J Fluid Mech*, vol. 376, pp. 221–261, Dec. 1998, doi: 10.1017/S0022112098002869.

[15] C. R. Hackney *et al.*, "The influence of flow discharge variations on the morphodynamics of a diffluence–confluence unit on a large river," *Earth Surf Process Landf*, vol. 43, no. 2, pp. 349–362, Feb. 2018, doi: 10.1002/ESP.4204.